UBV polarimetry of 361 A- and F-type stars in selected areas[*,**]

A. Reiz[1] and G.A.P. Franco[2]

[1] Niels Bohr Institute for Astronomy, Physics and Geophysics, Juliane Maries Vej 30, DK 2100, Copenhagen Ø, Denmark
[2] Departamento de Física, ICEx, UFMG, Caixa Postal 702, 30.161-970, Belo Horizonte, MG, Brazil

Abstract. We present simultaneous *UBV* linear polarization measurements for 361 A- and F-type stars with accurate colour excess and distance determination. These stars are distributed in 35 Kapteyn's Selected Areas, covering the third and fourth quadrants of the galactic plane ($|b| \leq 30°$). The obtained polarization and the known colour excess are compared. An analysis of the polarization distribution as a function of the stellar distance is also performed.

Key words: polarization — interstellar medium: dust, extinction — stars: general — catalogs

1. Introduction

The properties of the local interstellar medium has been probed by several different techniques. As a result, there are evidences that the solar vicinity is a relatively depleted volume with an irregular shape. Such volume is usually called the Local Bubble and may be surrounded, at least in some directions, by large interstellar structures composing the surface of other bubbles, like the Loop I Bubble which is seen toward the whole fourth galactic quadrant. Among the techniques usually used to investigate the interstellar medium one may mention the measurement of the linear polarization of starlight, one of the most readily observable phenomena arising from the partial alignment of the aspherical interstellar dust grains. Although the alignment mechanism is not fully understood, it is clear that the galactic magnetic field is responsible for

this alignment, with the long axes of the grains tending to become orientated perpendicular to the field lines.

The knowledge of the linear polarization of starlight is important because it provides information on grain properties and also on the galactic magnetic field. The distribution of polarization vectors with respect to galactic coordinates has been investigated by a number of authors (Axon & Ellis 1976, and references therein), of which the most extensive data sets are those published by Mathewson & Ford (1970) and Klare et al. (1972). On the other hand, high precision polarimetry has been used by some authors to investigate the nearby low column volume (Tinbergen 1982; Leroy 1993a).

In this paper we introduce *UBV* linear polarization measurements collected for 361 A- and F-type stars with accurate distance and colour excess determination. A search in the available literature showed that only five of them have previous polarimetric measurements.
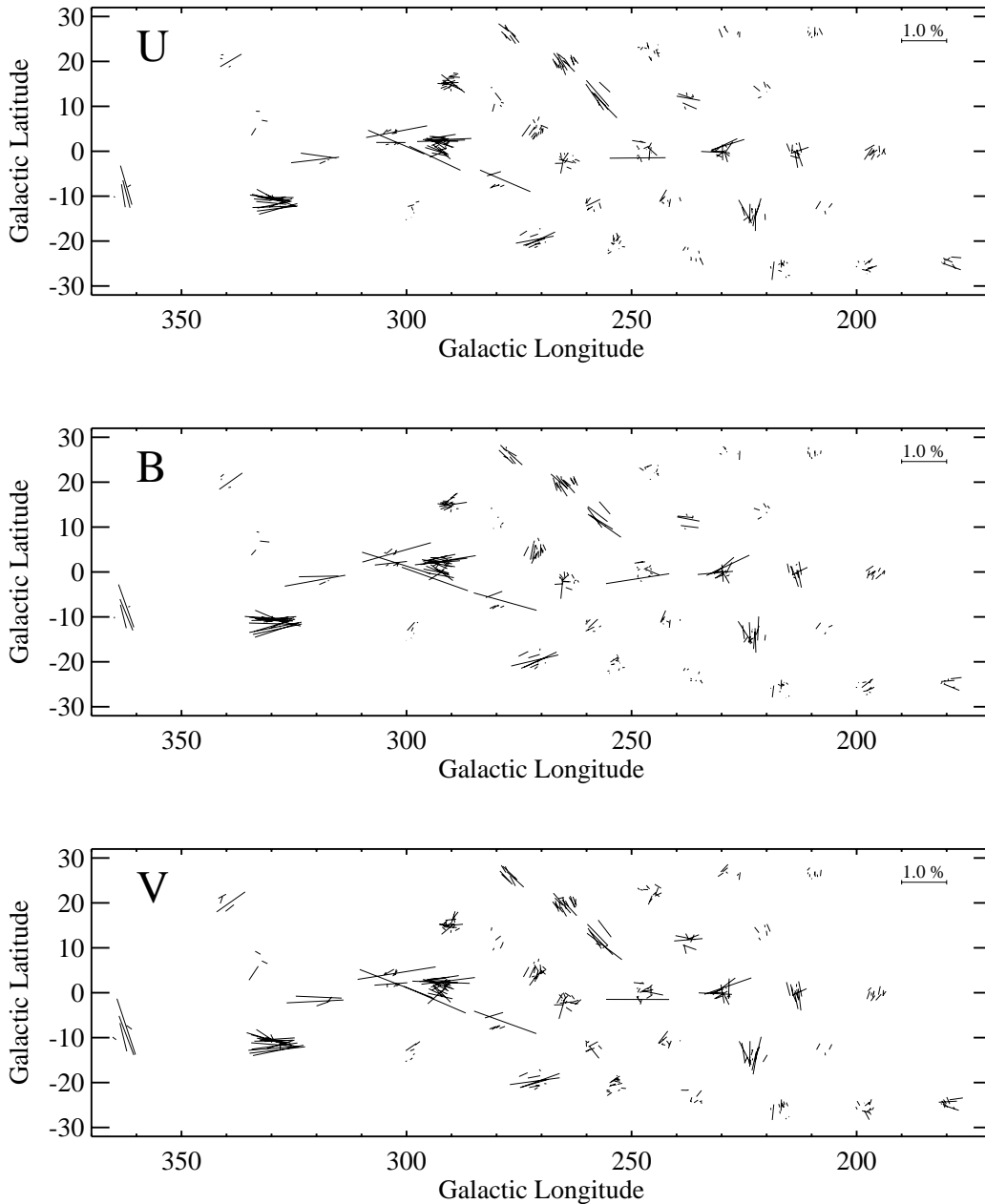
2. The observations

The observations were carried out at the Danish 1.5 m telescope at La Silla, on 10 nights in 1990 Jan. 08 – 17, 7 nights in 1991 Jan. 18 – 24, and 3 nights in 1992 Apr. 22 – 24. A multichannel version of the double image chopping polarimeter (Korhonen et al. 1984) was used, and the measurements in different colours were collected simultaneously by using dichroic filters to split the light into the spectral regions. The resulting passbands are close to the *UBV* system, with effective wavelengths 0.36, 0.44, and 0.54 μm, respectively. The sky background polarization was directly eliminated by using a plane parallel calcite plate as the polarizing beam splitter, and the intensities of the two beams are measured, for each colour, by a single photo-multiplier using chopping techniques (Piirola 1973). As determined from observations of unpolarized standard stars (Tinbergen 1979), the instrumental polarization was found to be very small. The zero point of position angles was determined by observations of seven standard stars with large interstellar polarization. These standard stars

Fig. 1. The $\boldsymbol{E}$-vectors of the UBV polarization measurements. The length of each line is proportional to P, the percentage polarization and the angle at which each line is drawn relative to the galactic north pole in the direction of increasing longitude is θ_{gal}

were selected from the list suggested by Serkowski (1974) and they were measured regularly throughout the observing periods. For most of the cases, the observation of one star took about 15 minutes and consisted of four sets of measurements at eight position angles of the instrument. At each position angle, integrations of 10 seconds were made for each one of the two light beams. In order to improve our accuracy, six sets of measurements were collected for some of the faintest stars.

The targets were selected from the Knude's A- and F-type star catalogue (Knude 1977, 1978). The observed stars belong to 35 low galactic latitude ($|b| \leq 30°$) Kapteyn's Selected Areas and cover the third and fourth quadrants of the galactic plane.

3. The results

The observed UBV polarimetric results are given in Table 1 (available in electronic form at the CDS via anonymous
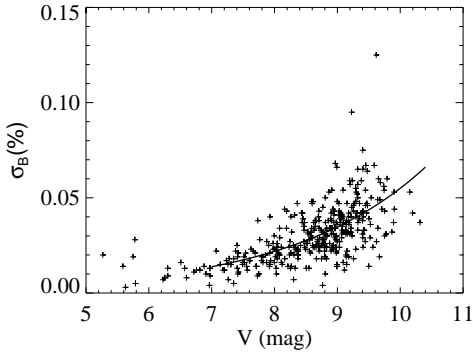
Fig. 2. Estimated error in the B-band versus stellar visual magnitude. The errors of bright stars ($V \lesssim 7\overset{\mathrm{m}}{.}0$) are mainly dominated by atmospheric scintillation. For fainter stars, it is dominated by photon shot noise and, in the present case, may be roughly represented by $\sigma_B = 5.5 \ 10^{-4} (10^V)^{1/5}$ (solid curve)

ftp to cdsarc.u-strasbg.fr (130.79.128.5)). The columns of this Table contain the following data:

Column 1: star identification in the Knude's catalogue;
Column 2: HD number, when available;
Column 3: right ascension for the equinox 1900.0;
Column 4: declination for the equinox 1900.00;
Column 5: galactic longitude;
Column 6: galactic latitude;
Column 7: computed V magnitude on the Johnson system (Knude 1977);
Column 8: measured polarization in the UBV bands in per cent, the respective estimated uncertainty is given between parenthesis;
Column 9: galactic position angle. This angle is measured relative to the galactic north pole in the direction of increasing longitude;
Column 10: equatorial position angle. This angle is measured relative to the celestial north pole in the direction of increasing right ascension. The respective estimated uncertainty is given between parenthesis;
Column 11: estimated colour excess ($E(b - y)$) (Knude 1978);
Column 12: estimated distance in parsecs (Knude 1978).

The measured polarizations are plotted in galactic coordinates in Fig. 1. The lines represent the **E**-vectors of the linearly polarized starlight. The lines are centered in the observed star's position. The length of each line is proportional to the percentage polarization and the angle at which each line is drawn relative to the galactic north pole in the direction of the increasing longitude is given by θ_{gal}.

The estimated average uncertainties of the polarimetric measurements are: $\overline{\sigma_U} = 0.048\%$, $\overline{\sigma_B} = 0.031\%$, and $\overline{\sigma_V} = 0.058\%$, respectively for the U, B, and V bands. Figure 2 displays the obtained uncertainties for the B-band as a function of the stellar magnitude. For bright stars ($V \lesssim 7\overset{\mathrm{m}}{.}0$) the uncertainty is mainly determined by atmospheric scintillation, and the mean uncertainty is

**Table 2.** Comparison between the polarization introduced in this work with previous measurements

star	$P_B\%$ this work	P literature	source
150 (HD 49933)	0.042	0.016	1
200 (HD 58461)	0.005	0.018	1
405 (HD 98310)	1.240	1.41	2
414 (HD 99545)	0.622	1.16	2
421 (HD 100198)	0.570	0.83	3

Sources:
  1. Leroy (1993b)   2. Klare & Neckel (1977)
  3. Mathewson & Ford (1970)

**Table 3.** Results obtained for the polarized standard stars

| star HD	$P_{\max}$ this work	$\lambda_{\max}$	$P_{\max}$ Serkowski (1974)	$\lambda_{\max}$
23512	2.20	0.59	2.3	0.60
43384	2.94	0.51	3.0	0.53
80558	3.30	0.58	3.3	0.61
84810	1.73	0.56	1.6	0.57
111613	3.11	0.54	3.2	0.56
147084	4.81	0.72	4.3	0.68
160529	7.35	0.55	7.3	0.54
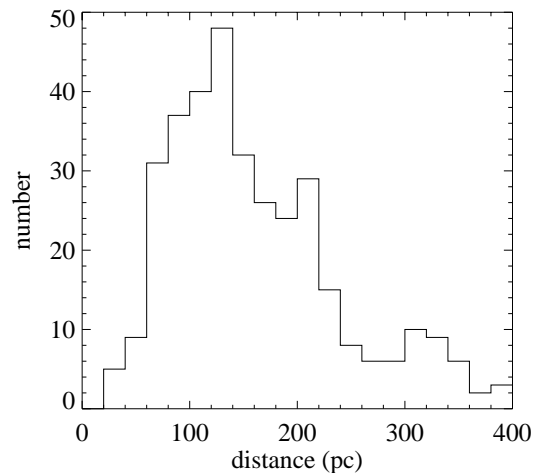
Fig. 3. The distribution of the observed stars as a function of the distance. Nineteen stars are located beyond the distance interval represented in this histogram

about $\pm 0.01\%$. For fainter stars, the uncertainty is dominated by photon shot noise, and since it has been used the same integration time to collect the measurements, the uncertainty increases as a function of the stellar magnitude.

Among the observed stars, 5 were found in the literature having previous polarimetric measurements. Table 2 gives a comparison between the polarization introduced in this work with the values found in the literature. Within the observational errors, a good agreement is obtained for the two unpolarized stars. The degree of polarization
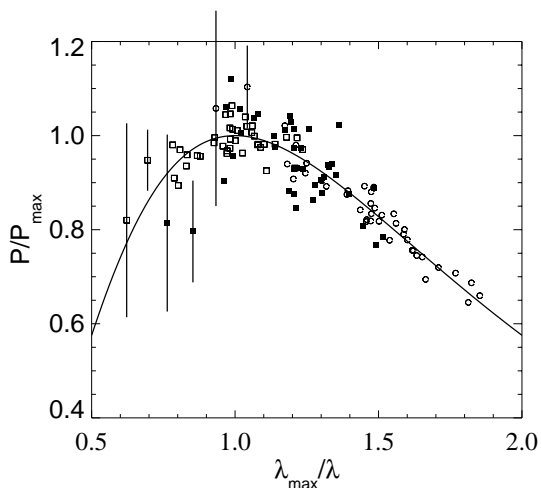
Fig. 4. The normalized wavelength dependence of the interstellar linear polarization derived from the 40 stars showing degree of polarization greater than 0.5% in all the observed passbands. The solid line represents the Serkowski's empirical formula relating the ratio P/P_{max} to the corresponding ratio λ_{max}/λ. The bars indicate the observed uncertainties for HD 79936 and HD 80085 (see text). The U, B, and V colours are represented by open circles, filled squares and open squares, respectively
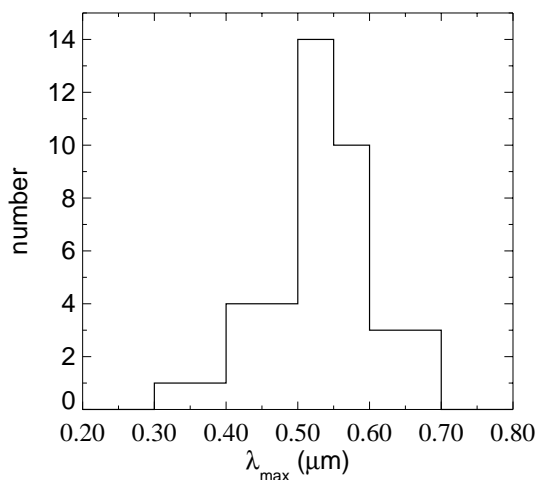
Fig. 5. The distribution of the obtained λ_{max} values for the 40 stars showing degree of polarization greater than 0.5% in all the observed passbands

obtained for the remaining polarized stars seems to be systematically smaller than the value found in the literature. In special, a rather large discrepancy was observed for the polarized star 414 (HD 99545). Such discrepancy requires a more careful analysis. In order to test the accuracy of our measurements for the polarized stars, we have compared the observed polarizations obtained for the standard stars used to determine the zero point of polarization angles with the standard values.

Table 3 gives a comparison between the results obtained from our measurements and the standard val-

ues. The maximum polarization (P_{max}) and the wavelength λ_{max} were obtained as described in the next section. The agreement between our results and the standard ones is very good. Except for the case of HD 147084, the difference for the maximum polarizations is smaller than 0.1%. An analysis of the measurements obtained for HD 147084 showed that the observed discrepancy is mainly caused by a difference in the polarization observed for the V channel, as compared to the value obtained by Serkowski et al. (1975).

An idea of the stellar distance distribution of the observed sample can be obtained by the histogram given in Fig. 3. Almost 70% of the stellar sample is closer than 200 pc. There are 19 stars located beyond the distance interval represented in this figure.

4. The observed wavelength dependence

It was noticed by Serkowski (1973) that observations of linear interstellar polarization follows the same curve when the ratio of polarizations $P(\lambda)/P(\lambda_{max})$ is plotted against the ratio of the wavelength λ_{max} of the maximum polarization for a given star to the wavelength λ at which polarization is measured. The Serkowski's empirical relationship is given by

$$P(\lambda)/P(\lambda_{max}) = \exp[-K \ln^2(\lambda_{max}/\lambda)], \qquad K = 1.15.$$

The wavelength of maximum polarization varies from star to star and is typically in the range 0.45 μm to 0.8 μm, with a median value of 0.545 μm (Serkowiski et al. 1975).

Least squares fit were applied to the 40 stars showing degree of polarization greater than 0.5% in the UBV passbands. From the obtained fit, the P_{max} and λ_{max} were found for each of these stars. Figure 4 gives a comparison between the obtained normalized wavelength dependence of the observed linear polarization (dots) with the Serkowski's formula (solid line).

Figure 5 shows the distribution of the obtained λ_{max}. The diagram shows a maximum in the range $0.50 < \lambda_{max} \leq 0.55 \,\mu$m. The median value for the obtained λ_{max} values is 0.534 μm, in agreement with what is observed for the typical interstellar medium. There are two stars ($315 -$ HD 79936 and $317 -$ HD 80085) showing rather small λ_{max} values, and since their lines-of-sight sit in the same region of the sky, the abnormal values may be characteristic of this direction. However, due to the uncertainties in the measurements, mainly for 315 (HD 79936), this hypothesis requires further confirmation.

5. Polarization versus reddening

As mentioned before, the observed sample contains stars for which distance and colour excess have been accurately determined. It is then instructive to compare the spatial distribution of the colour excess and polarization. It must be, however, noted that the polarization values listed in Table 1 are by definition positive quantities, which suffer
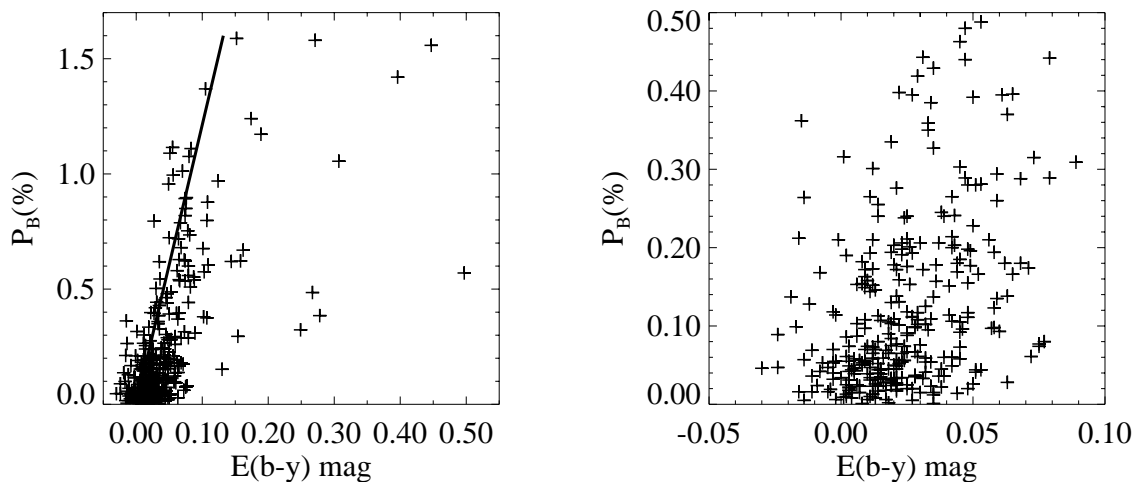
Fig. 6. The polarization in the B-band versus $E(b - y)$. (*left*) All observed stars. The solid line represents optimum alignment efficiency ($P(\%) = 12.1 \times E(b-y)$; $E(b-y) = 0.74\ E(B-V)$). (*right*) Expanded view for the low reddening part of the diagram

a positive bias which is not negligible at low polarization levels, while colour excess do not suffer the same effect.

Usually, it is observed that although polarization and extinction (reddening) occurs whenever stellar light is propagated through a medium containing small particles, the correlation between these two quantities is by no means perfect. While the reddening caused by successive clouds is always increasing, the polarization has a more complex behaviour. This fact is illustrated by diagrams where the interstellar polarization is represented against the reddening (e.g. Serkowski et al. 1975) which show that the ratio $P_{\max}/E_{B-V}$ rarely exceeds 9.0. Figure 6 (*left*) gives the polarization versus colour excess diagram for all observed stars. The straight line represents the above mentioned optimum alignment efficiency, which is reached under special conditions only. Figure 6 (*right*) gives an expanded view for the low reddening part of the polarization versus reddening diagram. As expected, there are several stars showing a ratio $P/E_{B-V} < 9.0$, but in general, most of the observed stars are distributed close to the optimum alignment line indicating a rather good correlation between these two quantities.

In Fig. 7 one can compare the distribution of polarization and colour excess as a function of the stellar distance. There are 32 stars up to a distance of 70 pc. This stellar group presents an average polarization of $\overline{P_B} = 0.03\%$, which is similar to the estimated mean error obtained for them ($\overline{\sigma_B} = 0.02\%$), and an average colour excess of $\overline{E}(b - y) = 0\overset{\mathrm{m}}{.}013$, which is also comparable to the expected mean error for the colour excess determination (Knude 1978). The obtained average polarization is ≈ 5 times smaller than the expected maximum polarization value for optimum alignment efficiency. This result enforces the fact that the solar neighbourhood is a low column density volume, at least when concerning the third

and fourth galactic quadrants, up to distances of about 70 pc. The colour excess diagram (Fig. 7 – lower) shows clear signs of the existence of interstellar dust at a distance of ≈ 60 pc. Figures 8–11 give a comparison between the spatial distribution of polarization and colour excess for four distance intervals. In the first interval ($d < 100$ pc), most of the observed stars are unpolarized and the few ones showing some degree of polarization also show some trace of reddening. On the other hand, in the second distance interval ($100 \leq d < 150$ pc) one clearly see the effects of the interstellar dust on the stellar light yielding polarization as well as reddening. The interstellar dust traced here may be related to a large structure defining the interface between the Local and Loop I Bubbles. An extensive study of reddening versus distance conducted by Corradi et al. (1997) suggested the existence of a continuous sheet structure extending from the Chamaeleon region towards the Coalsack ($294° \leq l \leq 308°$, $-18° \leq b \leq 5°$), at a distance of 150 ± 30 pc from the Sun, which has been associated to this interface.

References

Axon D.J., Ellis R.S., 1976, MNRAS 177, 499
Corradi W.J.B, Franco G.A.P., Knude J., 1997, A&A 326, 1215
Klare G., Neckel Th., Schnur G., 1972, A&AS 5, 239
Klare G., Neckel Th., 1977, A&AS 27, 215
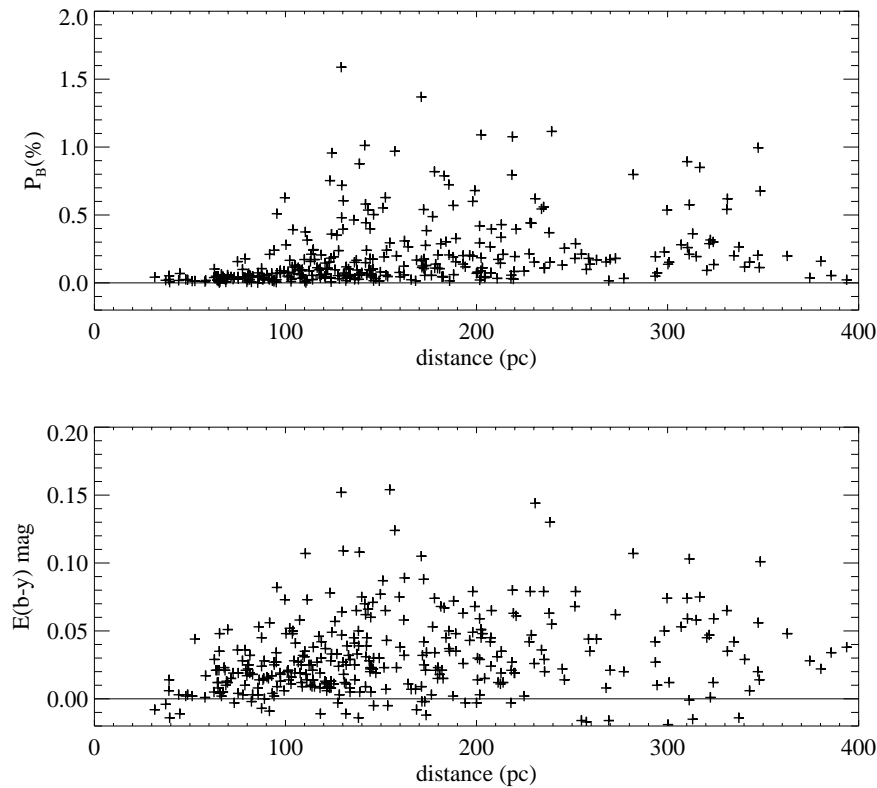
Fig. 7. (*upper*) The polarization in the B-band versus distance. (*lower*) $E(b-y)$ versus distance. Although polarization is a positive quantity, the vertical axis of the upper diagram has been extended to negative values in order to make easier the comparison between both diagrams. It is remarkable, nevertheless the positive bias, the small degree of the observed linear polarization showed by stars up to ≈ 100 pc

Knude J., 1977, A&AS 30, 297
Knude J., 1978, A&AS 33, 347
Korhonen T., Piirola V., Reiz A., 1984, The ESO Messenger 38, 20
Leroy J.L., 1993a, A&A 274, 203
Leroy J.L., 1993b, A&AS 101, 551
Mathewson D.S., Ford V.L., 1970, Mem. R. Astron. Soc. 74, 139
Piirola V., 1973, A&A 27, 383

Serkowski K., 1973, in "Proc. IAU Symp. 52: Interstellar Dust and Related Topics", Greenberg J.M. and van de Hulst H.C. (eds). Dordrecht, Reidel, p. 145
Serkowski K., 1974, in "Planets, stars, and nebulae studied by photopolarimetry". Gehrels T. (ed.). The University of Arizona Press, Tucson, U.S.A., p. 135
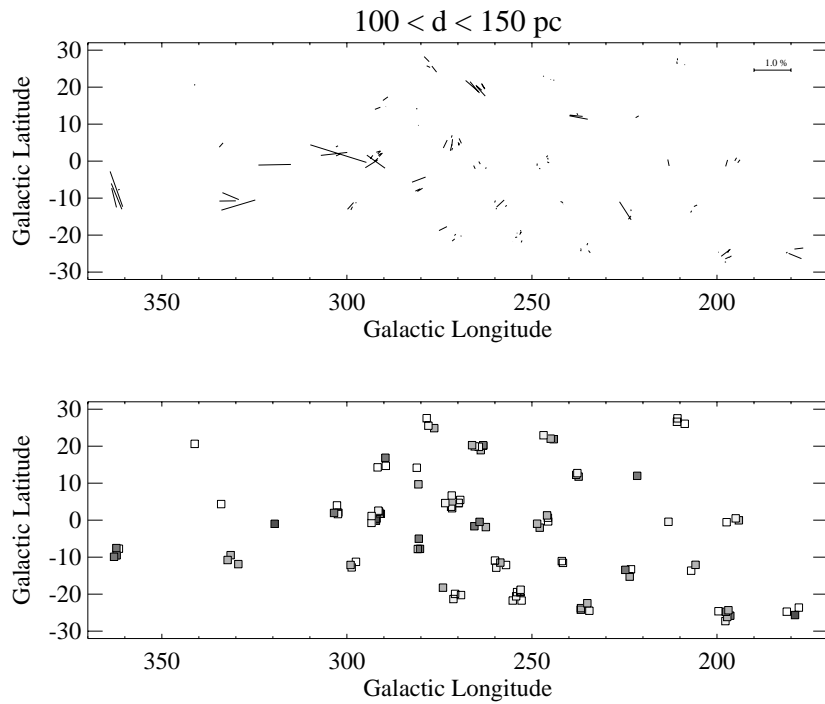Serkowski K., Mathewson D.S., Ford V.L., 1975, ApJ 196, 261
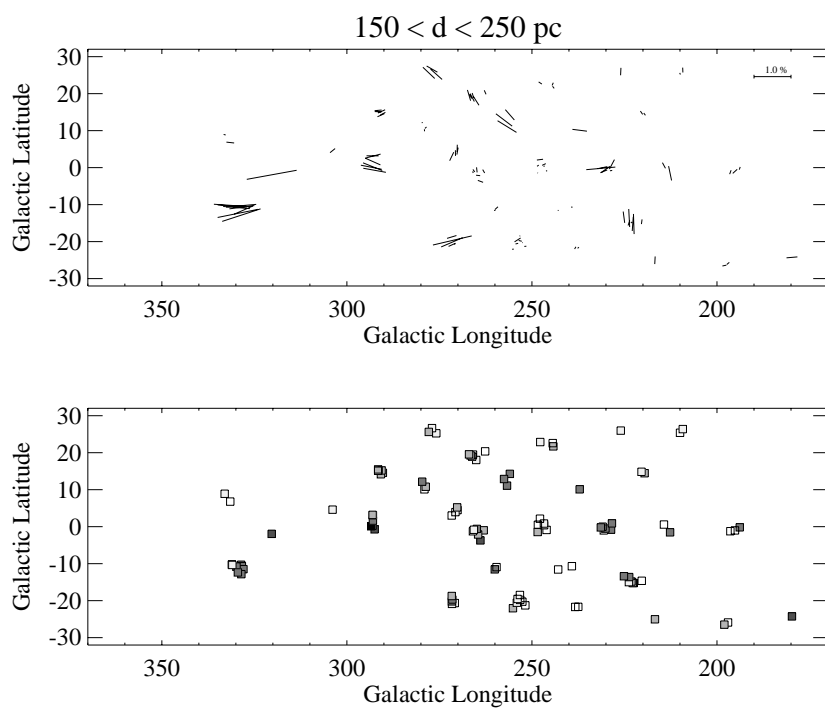Tinbergen J., 1979, A&AS 35, 325
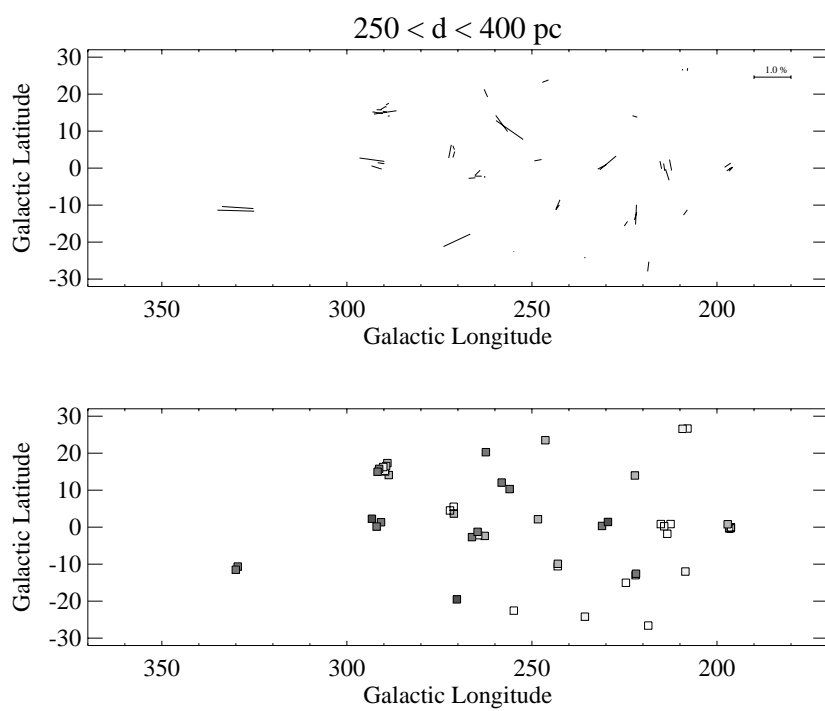Tinbergen J., 1982, A&A 105, 53
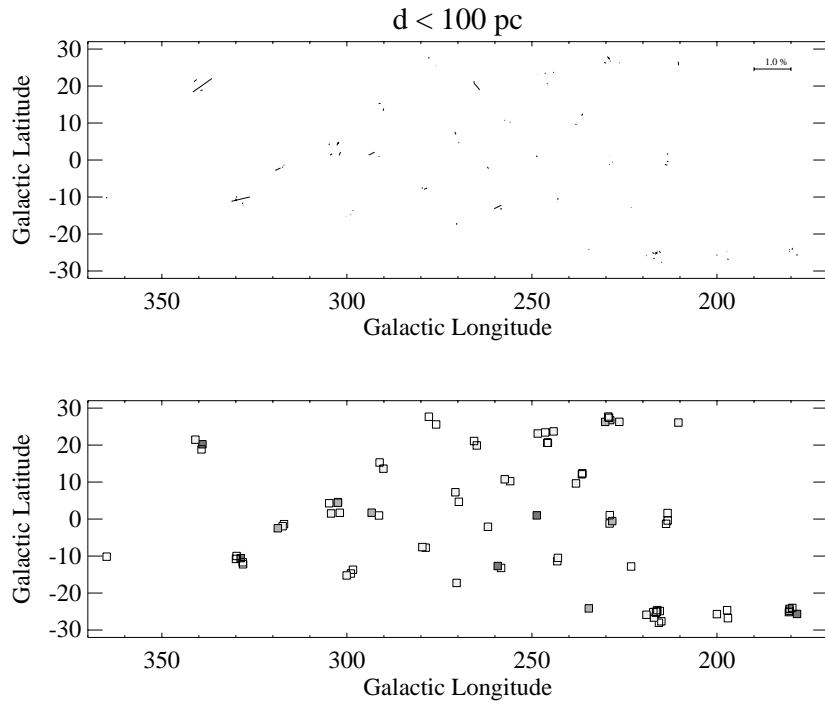
Fig. 8. Observed polarization (B-band) and colour excess $E(b-y)$ up to 100 pc. The estimated colour excess are indicated by the small squares as: (☐) $E(b-y) < 0\overset{m}{.}017$. (☐) $0\overset{m}{.}017 \leq E(b-y) < 0\overset{m}{.}030$. (☐) $0\overset{m}{.}030 \leq E(b-y) < 0\overset{m}{.}050$. (■) $0\overset{m}{.}050 \leq E(b-y) < 0\overset{m}{.}100$. (■) $0\overset{m}{.}100 \leq E(b-y) < 0\overset{m}{.}200$. (■) $E(b-y) \geq 0\overset{m}{.}200$

Fig. 9. Same as Fig. 8. Stars in the range $100 \leq d < 150$ pc

Fig. 10. Same as Fig. 8. Stars in the range $150 \leq d < 250$ pc

Fig. 11. Same as Fig. 8. Stars in the range $250 \leq d < 400$ pc